ACS OMEGA

Open Access

http://pubs.acs.org/journal/acsodf

Article

Wood-Derived Ionic Conductive Cellulose for Transparent and Flexible Methamphetamine Analog Sensors

Brian Zhao,[§] Chenghao Wang,[§] Jia Huang, and Junyao Zhang*

Cite This: *ACS Omega* 2025, 10, 17770−17776

Read Online

ACCESS | Metrics & More | Article Recommendations | Supporting Information

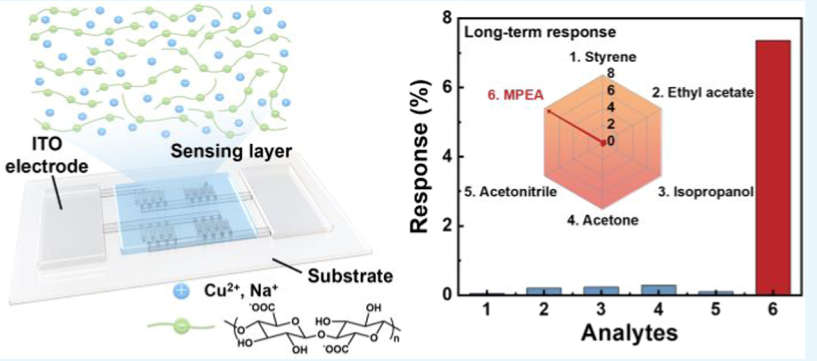

ABSTRACT: Developing covert, convenient, rapid, and cost-effective detection methods for trace amounts of addictive drugs poses a challenging task. Herein, wood-derived ionic conductive cellulose (WICC) is presented as a sensitive material, where active metal cations serve as charge carriers and effective adsorption/binding sites for a typical analog of the addictive drug *N*-methylphenethylamine (MPEA). The addition of Cu^{2+} ions improves the sensing performance of WICC, and the simple drop-coating process will facilitate the fabrication of the device array and the integration with flexible substrates. Taking advantage of WICC with excellent ion conductivity, high transparency, and mechanical flexibility, transparent and flexible sensors based on WICC are demonstrated, enabling real-time detection of MPEA. Notably, the high transparency makes WICC particularly suitable for covert detection. More significantly, the WICC sensors exhibit outstanding selectivity, facilitating an ultralow theoretical detection limit (∼12 nL). This work provides a promising pathway toward the next-stage construction of invisible chemical sensors for addictive drug detection.

INTRODUCTION

The illegal abuse of addictive drugs has currently become a global issue, posing enormous threats to human health.[1] Specifically, ingesting even trace amounts of addictive drugs can cause irreversible damage to vital organs. Hence, it is an urgent priority to develop sensitive, real-time, and cost-effective technologies to detect trace amounts of addictive drugs. Methamphetamine is a commonly used addictive drug.[2] However, due to restrictions on the availability of methamphetamine, a substitute known as *N*-methylphenethylamine (MPEA) with similar structure and chemical properties is commonly utilized as an analog for methamphetamine in detection analyses.[3] Presently, conventional analytical methods for detecting MPEA frequently rely on advanced spectroscopic and biophysical technologies.[4−6] Despite their advantages in sensitivity and accuracy, these technologies are normally hindered by high costs, bulky equipment, and complex sample preparation, which limit their further applicability in rapid, real-time, and covert detection scenarios.

Chemical sensors have emerged as one type of promising practical equipment for detecting addictive drugs due to their portability and sensitivity.[7−9] Most of the currently available chemical sensors interact with target analytes based on redox reactions or charge transfer/trapping, which rely on holes or electrons as charge carriers.[10−12] These chemical sensors rely on various sensitive materials, such as metal oxides,[13] carbon-based materials,[14,15] and organic polymers,[16] to achieve the detection of target substances. Despite their wide detection range and good stability, these sensors commonly suffer from relatively low sensitivity and poor selectivity and sometimes require a high operating temperature. In contrast, chemical sensors based on ionic conductive materials demonstrate irreplaceable application potentials, including room-temperature operation capability, excellent selectivity, and high

Received: January 9, 2025
Revised: February 24, 2025
Accepted: April 11, 2025
Published: April 21, 2025

https://doi.org/10.1021/acsomega.5c00235
ACS Omega 2025, 10, 17770−17776

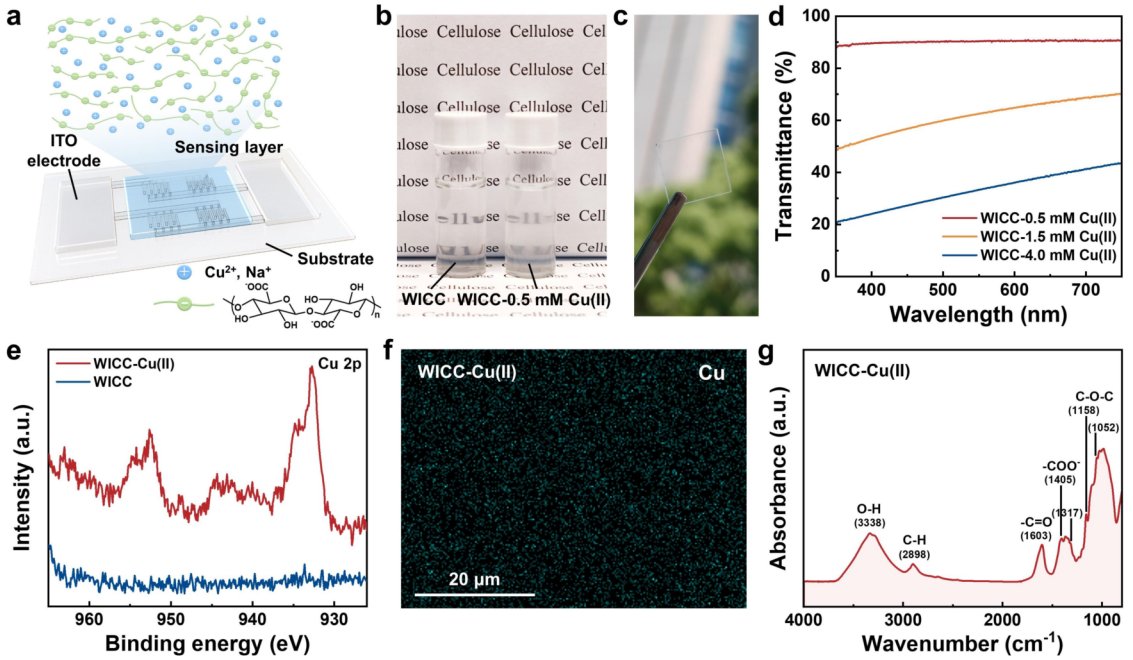

Figure 1. (a) Schematic diagram of the WICC-Cu(II) sensor. (b) Photo of the WICC solution and WICC-0.5 mM Cu(II) solution. (c) Photo of the WICC-0.5 mM Cu(II) film deposited on quartz glass. (d) Transmittance of the WICC-Cu(II) films with different Cu^{2+} concentrations. (e) Cu 2p spectra of the WICC film and WICC-Cu(II) film. (f) Distribution of the Cu element in the WICC-Cu(II) film obtained from EDS analysis. (g) The FTIR spectrum of the WICC-Cu(II) film.

stability.[17,18] Among this kind of sensor, active free ions play a key role as effective charge carriers. For example, for ionogel-based sensors, ionic liquids can be used as charge carriers,[19−21] and for MOF-based sensors, metal ions can be used as charge carriers.[22,23] These charge carriers interact with the target substances and eventually convert them into readable signals. To further employ sensors in the field of addictive drug detection, it is crucial to consider the concealment of sensors, which is also a key aspect overlooked by most chemical sensors. Therefore, the development of transparent and intelligent chemical sensors reliant on novel ionic conductive materials can be used to effectively address the shortcomings of existing methods for detecting addictive drugs and also meet national security and public health requirements, thus demonstrating their broad prospects of practical applications.[24]

Cellulose, a key component of wood, has increasingly become a research focus in green electronics owing to its unique merits, such as natural abundance, mechanical flexibility, biodegradability, and biocompatibility.[25−27] Previous studies have found that nanofibrillated cellulose obtained from wood-derived cellulose via (2,2,6,6-tetramethylpiperidin-1-yl)-oxidanyl (TEMPO) treatment, also known as WICC, exhibits both good transparency and flexibility.[28,29] Additionally, due to the introduction of sodium ions during the TEMPO treatment, WICC also demonstrates excellent ion conductivity.

Here, leveraging the merits of WICC, this work developed portable, transparent, and flexible sensors based on WICC as the ionic conductive material for detecting trace amounts of MPEA. Using active metal ions as charge carriers, a small amount of copper ions (Cu^{2+}) were introduced into WICC (abbreviated as WICC-Cu(II)) to further enhance the sensitivity and selectivity of the WICC-based sensors. The WICC-Cu(II) sensitive material maintained high transmittance (>87%) in the visible light range. Benefiting from irreversible and specific responses of the WICC-Cu(II) sensors to MPEA, the sensors demonstrated high selectivity. Furthermore, the sensors exhibited other outstanding detection capabilities for MPEA at room temperature, including low detection volume (0.02 μL) and an ultralow theoretical detection limit (LOD, 12 nL). More significantly, the flexible WICC-Cu(II) sensors maintained detection performance comparable to the initial state even after 1000 bending tests, demonstrating the feasibility of integrating them into various portable and wearable electronics. The proposed transparent and flexible sensors based on green WICC material provide a new approach to developing invisible chemical sensors for the detection of addictive drugs.

RESULTS AND DISCUSSION

Figure 1a depicts the schematic diagram of the WICC-Cu(II) sensor, where WICC-Cu(II) serves as the sensitive material and is dropped onto the patterned electrodes, indium tin oxide (ITO) functions as the highly transparent patterned electrodes, and glass/poly(ethylene terephthalate) (PET) acts as rigid/flexible transparent substrates. The WICC-Cu(II) films, with differing Cu^{2+} concentrations, were obtained by blending varying amounts of $Cu(NO_3)_2$ solution with the WICC suspension synthesized through TEMPO treatment (Figure S1). Due to the decrease in transparency of the WICC-Cu(II) film caused by the introduction of Cu^{2+}, the influence of different Cu^{2+} concentrations on the transparency of WICC-Cu(II) was first examined in an effort to balance the ion conductivity and the transparency of the WICC-Cu(II) film. As depicted in Figures 1b−c and S2, the transparency of the WICC solution with a concentration of 0.5 mM Cu^{2+} (abbreviated as WICC-0.5 mM Cu(II)) exhibited almost no decrease compared with the pure WICC solution. However, further increasing the concentration of Cu^{2+} in the WICC solution resulted in a notable decrease in transparency, which might be attributed to the aggregation or precipitation of

https://doi.org/10.1021/acsomega.5c00235
ACS Omega 2025, 10, 17770−17776

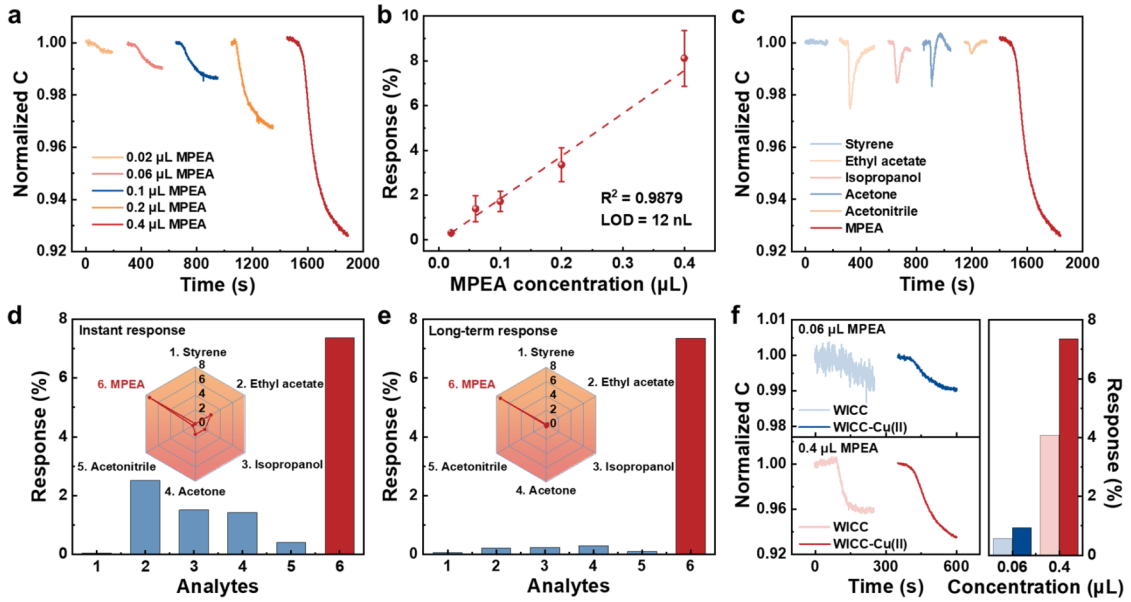

Figure 2. (a) Responses of the WICC-Cu(II) sensor to different concentrations of MPEA. (b) The corresponding relationship between the responses and MPEA concentrations. (c) Responses of the WICC-Cu(II) sensor to MPEA and interfering substances with the same concentration. (d) Instant responses and (e) long-term responses to MPEA and interfering substances. (f) Comparison of the responses of the WICC sensor and WICC-Cu(II) sensor to different concentrations of MPEA.

WICC induced by excessive divalent metal ions.[30] The transparency of the WICC-Cu(II) films with different Cu^{2+} concentrations was further investigated. As depicted in Figure 1d, the WICC-0.5 mM Cu(II) film showed a high transmittance (>87%) in the visible range. With the increase of Cu^{2+} concentration in the WICC, the transparency of the WICC-Cu(II) film obviously decreased. Thus, to meet the invisible requirement of the sensors in practical applications, the WICC-0.5 mM Cu(II) solution was chosen as the precursor for the sensing layer in this work, and WICC-0.5 mM Cu(II) was abbreviated as WICC-Cu(II) below.

To validate the successful introduction of Cu^{2+} into the WICC, X-ray photoelectron spectroscopy (XPS) was employed. As depicted in Figure 1e, the Cu 2p spectrum of the WICC-Cu(II) film exhibited new characteristic peaks compared with those of the WICC film. Besides, energy-dispersive spectroscopy (EDS) was also utilized to validate the homogeneous distribution of Cu^{2+} within the WICC film. As depicted in Figure 1f, the Cu element was uniformly dispersed in the film, proving the efficacy of the WICC-Cu(II) sensing layer. In addition, the uniform distribution of the Na element was observed in the WICC-Cu(II) film (Figure S3). Figure 1g depicts the Fourier transform infrared (FTIR) spectrum of the WICC-Cu(II) film. The characteristic peaks of the WICC-Cu (II) film were quite similar to those of the WICC film (Figure S4), indicating that the introduction of Cu^{2+} had no significant impact on the structure of WICC.[17] Likewise, the scanning electron microscopy (SEM) image of the WICC-Cu(II) film demonstrated its uniform surface, which also ensured the high transparency of the film (Figure S5). Briefly, the WICC-Cu(II) film can be simply prepared through the solution method without causing the aggregation of WICC or metal ions, further guaranteeing the sensing performance and transparency of the WICC-Cu(II) sensors.

To evaluate the sensing performance of the WICC-Cu(II) sensors, the devices were enclosed in a chamber connected with an LCR meter to examine the responses to different concentrations of the detection target MPEA. First, the responses of WICC-Cu(II) sensors to the same concentration of MPEA at different temperatures and humidity were investigated. Figure S6a demonstrates the responses of the WICC-Cu(II) sensors to MPEA at different humidity. It can be seen that when the relative humidity (RH) was set at 50%, the sensors demonstrated a maximum response. However, when the RH was set at 23 and 50%, the noise of the baseline was relatively high (Figure S6c–S6d), which could be attributed to the relatively small capacitance of the sensor. Figure S6b demonstrates the responses of the WICC-Cu(II) sensors to MPEA at different temperatures. As depicted in Figure S6e–S6g, the response of the sensor significantly increased at 35 °C, compared to the response at room temperature (~22 °C). When the temperature was set at 45 °C, the response of the sensor was still higher than that at room temperature, while the noise of the curve also became more pronounced. In summary, the WICC-Cu(II) sensor exhibited an optimal signal-to-noise ratio at RH of 75% and within the temperature range of ~22 to 35 °C. Therefore, unless otherwise noted, the sensors were evaluated at RH of 75% and room temperature of ~22 °C.

Then, the responses of the sensors to different concentrations of MPEA were investigated. As shown in Figure 2a, once exposed to specific concentrations of MPEA, the capacitance of the devices rapidly decreased and then gradually reached a stable status. As the concentration of MPEA increased, the response of the devices to MPEA increased. Notably, even when the devices were exposed to an extremely low concentration of MPEA (0.02 μL), an obvious response was still observed. Considering the volatilization process of MPEA, the lower concentration of MPEA corresponds to a faster response time. Moreover, the response of the devices to MPEA was almost linearly related to the MPEA concentration (Figure 2b). As a result, the LOD was calculated to be ~12 nL, which demonstrated the high sensitivity and low detection limit of the WICC-Cu(II) sensors. It is noteworthy that after

https://doi.org/10.1021/acsomega.5c00235
ACS Omega 2025, 10, 17770−17776

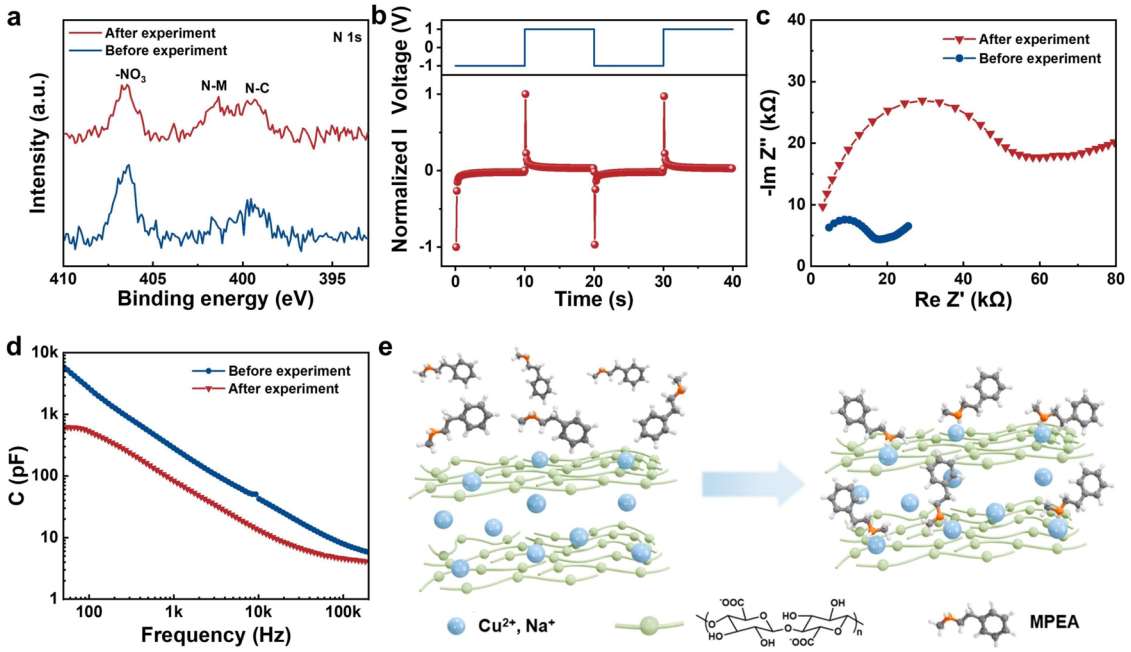

Figure 3. (a) N 1s spectra of the WICC-Cu(II) film before and after exposure to MPEA. (b) *I*−*t* curve of the WICC-Cu(II) sensor. (c) Nyquist plots of the WICC-Cu(II) film before and after exposure to MPEA. (d) Capacitance−frequency curve of the WICC-Cu(II) sensor before and after being exposed to MPEA. (e) Schematic diagram of sensing mechanism of the WICC-Cu(II) sensor to MPEA.

the devices were exposed to MPEA, the capacitance of the devices did not recover to the initial state, exhibiting irreversible responses.

In order to evaluate the anti-interference capability of the WICC-Cu(II) sensors, different interfering substances (including styrene, ethyl acetate, 2-propanol, acetone, and acetonitrile) with the same concentration were utilized. As depicted in Figure 2c, when exposed to the interfering substances, the capacitance of the devices rapidly decreased and then nearly recovered to the initial state. For all of the tested interfering substances, the devices exhibited small, short-term, and reversible responses, which were completely different from the responses to MPEA (Figure 2d−e). The diverse responses to different substances suggest that the WICC-Cu(II) sensors have a weak interaction capability with the mentioned interfering substances but a strong interaction capability with MPEA, demonstrating the excellent anti-interference characteristic of the sensors. This further enables the WICC-Cu(II) sensors to well recognize the presence of MPEA even under complex detection conditions and demonstrates great potential for practical addictive drug detection.

To prove the effect of the introduction of Cu^{2+} into WICC on the detection capability, the responses of the WICC sensors to MPEA were investigated. As depicted in Figures 2f and S7, the WICC sensors also exhibited irreversible responses to MPEA, and a relatively linear relationship between the response and MPEA concentration was still obtained. However, compared to the WICC-Cu(II) sensors, the WICC sensors revealed smaller responses with a larger noise. The decreased noise in the WICC-Cu(II) sensors can be attributed to the introduction of Cu^{2+}, which raises the content of conductive ions in the sensing layer and subsequently increases the basic capacitance of the devices. Furthermore, when exposed to 0.06 μL MPEA, almost no apparent response was achieved in the WICC sensor, while an obvious response could still be obtained in the WICC-Cu(II) sensor. Besides, when the concentration of MPEA increased to 0.4 μL, the response of the WICC-Cu(II) sensor enhanced by 80% compared with that of the WICC sensor. Thus, the presence of Cu^{2+} can not only improve the response of sensors but also decrease the detection limit to MPEA. To further reveal the sensing mechanism of the WICC-Cu(II) sensor, XPS was further employed. As depicted in Figure 3a, $-NO_3$ came from the introduction of nitrate ions caused by the $Cu(NO_3)_2$ solution.[31] After being exposed to MPEA, a new peak corresponding to N-metal ions (N-M) was observed, which could be attributed to the interaction of the metal ions (M = Cu^{2+}, Na^+) present in the WICC-Cu(II) layer with MPEA.[32] The formation of the N-M structure explains the irreversible responses of the devices to MPEA. In contrast, due to the absence of N-M structure formation, the above-interfering substances may not stably interact with the sensing layer, resulting in small and reversible responses. In addition to the N 1s spectra of the WICC-Cu(II) film, no significant variation was observed in the Cu 2p spectra and Na 1s spectra before and after the exposure to MPEA (Figure S8).

To validate the ion conductivity characteristic of the WICC-Cu(II) film, DC voltage sequences were employed for the sensors (Figure 3b). When a positive voltage of 1 V was applied, the current of the devices decreased in a short period of time. Subsequently, when a negative voltage of −1 V was applied, the reverse current was also rapidly reduced. This phenomenon proves the ion conductivity property of the sensitive material.[33] Furthermore, the Nyquist plot indicates that the impedance of the WICC-Cu(II) sensors after exposure to MPEA was higher than that before exposure (Figure 3c). Due to the ion conductivity characteristic of the WICC-Cu(II) film, the higher impedance means fewer mobile ions within the sensors. The metal ions in the sensing layer interact with MPEA, which reduces the concentration of mobile ions, thereby leading to a decrease in the capacitance of the devices. As the testing frequency increased, the capacitance of the

https://doi.org/10.1021/acsomega.5c00235
ACS Omega 2025, 10, 17770−17776

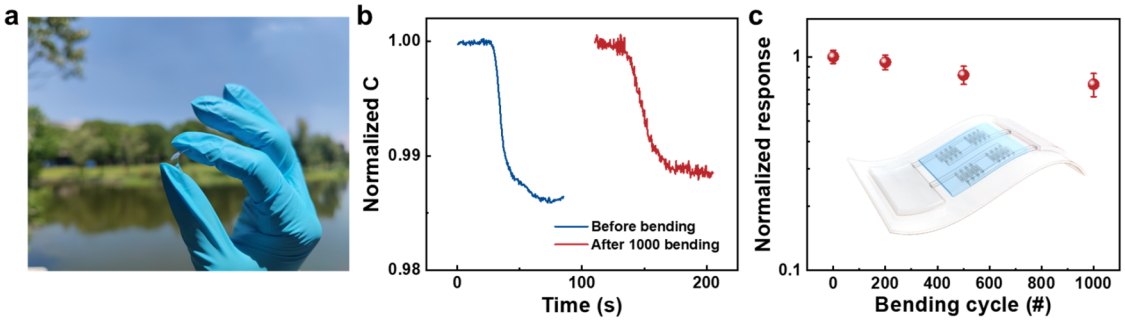

Figure 4. (a) Photo of the flexible WICC-Cu(II) sensor. (b) Responses of the flexible WICC-Cu(II) sensor to MPEA before and after 1000 bending cycles. The bending radius was 6 mm. (c) Comparison of the responses of the flexible WICC-Cu(II) sensor to MPEA before and after different bending cycles. The bending radius was 6 mm. The inset is a schematic diagram of the flexible WICC-Cu(II) sensor.

devices before and after exposure to MPEA decreased (Figure 3d). When the testing frequency was 50 Hz, the initial capacitance of the WICC-Cu(II) sensor reached up to 5.7 nF, while only the capacitance of 0.58 nF was achieved after the WICC-Cu(II) sensor was exposed to MPEA. These results reveal that the WICC-Cu(II) sensors own a high initial capacitance and can be operated within a wide frequency range.

Moreover, Figure 3e briefly depicts the sensing mechanism of the WICC-Cu(II) sensor to MPEA. In short, before contact with MPEA, metal cations in WICC, such as Cu^{2+} and Na^{+}, can move in the cellulose network, providing the basic capacitance of the sensor. After contact with MPEA, MPEA will bind with some metal cations in WICC due to the presence of −NH groups in MPEA, hindering the movement of ions and ultimately leading to a decrease in the capacitance of the sensor. Additionally, the sensing characteristics between the WICC-Cu(II) sensor and other reported methamphetamine sensors were compared. As depicted in Table S1, most reported sensors focused on detecting drugs in solution, while our WICC-Cu(II) sensors could directly detect trace MPEA in gas and exhibited a relatively low detection limit.

Benefiting from the intrinsic flexibility of the WICC-Cu(II) film, a flexible WICC-Cu(II) sensor was fabricated based on the PET substrate with patterned ITO electrodes. As depicted in Figure 4a, the flexible WICC-Cu(II) sensor still exhibited high transparency. After 1000 bending cycles, the noise of the sensor slightly increased, which might be due to the slight deterioration of the contact between the WICC-Cu(II) film and ITO electrodes (Figure 4b). After a series of bending times, almost no significant response attenuation was observed (Figure 4c), indicating the outstanding flexibility of the WICC-Cu(II) sensors.

■ CONCLUSIONS

In summary, we have demonstrated transparent and flexible sensors based on WICC-Cu(II) as the ionic conductive material for detecting MPEA. Benefiting from exceptional ion conductivity, the WICC-Cu(II) sensors exhibited excellent selectivity, ultralow LOD (∼12 nL), and flexibility performance. The achievement of flexible WICC-Cu(II) sensors suggests a new avenue for the development of transparent chemical sensors for detecting addictive drugs.

■ EXPERIMENTAL SECTION

Materials. Copper nitrate trihydrate ($Cu(NO_3)_2{\cdot}3H_2O$), sodium hypochlorite (NaClO) solution, and (2,2,6,6-tetramethylpiperidin-1-yl)-oxidanyl (TEMPO) were purchased from Adamas, Aladdin, and Sigma-Aldrich, respectively. The size of the glass substrates and PET substrates was 15 mm × 15 mm, respectively. The conductive channel length and width of ITO patterned electrodes were 100 and 1000 μm, respectively.

Preparation of WICC-Cu(II) Sensing Layers. The WICC suspension was prepared via TEMPO treatment based on the previous report.[17,18] Quantitative $Cu(NO_3)_2{\cdot}3H_2O$ powders were dissolved in deionized water to prepare metal-ion solutions (100 mM). Then, 0.25 g of the WICC suspension, metal-ion solution (0, 10, 30, and 80 μL), and deionized water (1.75, 1.74, 1.71, and 1.67 mL) were mixed together, and then the mixed solutions were stirred for 2 h to obtain uniform solutions. Before the mixed solutions were drop-coated onto the substrates modified with ITO electrodes, the substrates were pretreated with surface plasma for 8 min to enhance hydrophilicity and adhesion and remove surface impurities. Finally, the substrates were exposed at room temperature for 12 h to cure the sensing layer.

Characterization. SEM and EDS (Nova Nano SEM 450) were utilized to obtain the surface morphology of the WICC-Cu(II) film and the distribution of elements in the WICC-Cu(II) film, respectively. FTIR spectroscopy (EQUINOX 55) was utilized to characterize the chemical structure of the WICC/WICC-Cu(II) film. XPS (ESCALAB 250Xi) was applied to investigate the chemical composition of the WICC/WICC-Cu(II) film and the changes before and after exposure to MPEA. UV−vis spectrometer (Agilent Technologies Co., Ltd., Cary 60) was employed to obtain the transparency of the WICC-Cu(II) film. The effective capacitance of the WICC-Cu(II) film was observed by an LCR meter (Tonghui TH2827C). The impedance of the WICC-Cu(II) film was achieved by an electrochemical station (Biologic SAS, VMP-3).

For the sensing test, the devices were completely enclosed in a chamber. For humidity testing, calcium chloride and saturated salt solutions were used to reduce and increase the humidity, respectively. For temperature testing, heating elements were used to control the different temperatures. The LCR meter was used to collect the detection signals with a frequency of 400 Hz. The flat-mouth crocodile clips were used to connect the LCR meter and ITO electrodes. Before testing, the devices remained stationary until the baseline stabilized. A certain amount of the MPEA was injected into the chamber using a syringe, which rapidly evaporated into gas by heating. Upon contact with the MPEA, the devices exhibited a change in capacitance. After that, the MPEA gas in the chamber

https://doi.org/10.1021/acsomega.5c00235
ACS Omega 2025, 10, 17770−17776

gradually diluted until it returned to the atmospheric environment before the next testing. The obtained raw data were normalized and converted into normalized responses using Formula 1

$$\frac{\Delta C_P}{C_0} = \frac{C_0 - C_P}{C_0} \times 100\% \quad (1)$$

where C_0 and C_p represent the capacitance values at the initial and measurement stages, respectively. ΔC_p serves as the changes in the capacitance values from C_0 to C_p.[14] Besides, the LOD was calculated by Formula 2[34,35]

$$3 \times \mathrm{RMS} = \mathrm{slope} \times \mathrm{LOD} \quad (2)$$

where RMS represented the root-mean-square deviation.

■ ASSOCIATED CONTENT

Supporting Information

The Supporting Information is available free of charge at https://pubs.acs.org/doi/10.1021/acsomega.5c00235.

Reaction formula of the WICC; photo of the WICC-0.5/1.5/4.0 mM Cu(II) solution; the distribution of Na element in the WICC-Cu(II) film; FTIR spectrum and of the WICC film; SEM image of the WICC-Cu(II) film; responses of the WICC-Cu(II) sensor at different humidity and temperatures; responses of the WICC sensor to different concentrations; XPS spectra of the WICC-Cu(II) film before and after being exposed to MPEA; and comparison of sensing characteristics between the WICC-Cu(II) sensor and other reported methamphetamine sensors (PDF)

■ AUTHOR INFORMATION

Corresponding Author

Junyao Zhang − *School of Materials Science and Engineering, Tongji University, Shanghai 201804, China;* orcid.org/0000-0002-6300-5875; Email: jyzhang0819@outlook.com

Authors

Brian Zhao − *Scarsdale High School, Scarsdale, New York 10583, United States*

Chenghao Wang − *School of Materials Science and Engineering, Tongji University, Shanghai 201804, China*

Jia Huang − *School of Materials Science and Engineering, Tongji University, Shanghai 201804, China;* orcid.org/0000-0002-2873-7704

Complete contact information is available at: https://pubs.acs.org/10.1021/acsomega.5c00235

Author Contributions

§B.Z. and C.W. contributed equally to this work.

Notes

The authors declare no competing financial interest.

■ ACKNOWLEDGMENTS

This work was supported by the National Natural Science Foundation of China (62374115). The authors also thank the characterization and testing center of School of Materials Science and Engineering at Tongji University for materials characterization.

■ REFERENCES

(1) Zhang, M.; Zhao, D.; Zhang, Z.; Cao, X.; Yin, L.; Liu, Y.; Yuan, T. F.; Luo, W. Time perception deficits and its dose-dependent effect in methamphetamine dependents with short-term abstinence. *Sci. Adv.* **2019**, *5*, No. eaax6916.

(2) Langone, D.; Painter, B.; Nash, C.; Hulshof, J.; Oldenhof, S.; Johnston, M. R.; Kirkbride, K. P. Impurity profiling of methamphetamine synthesized from methyl alpha-acetylphenylacetate. *Drug Test. Anal.* **2022**, *14*, 1310−1324.

(3) Li, K.; Wang, L.; Chen, J.; Yan, M.; Fu, Y.; He, Q.; Cheng, J. Detecting methylphenethylamine vapor using fluorescence aggregate concentration quenching materials. *Sens. Actuators, B* **2021**, *334*, No. 129629.

(4) Morita, I.; Kiguchi, Y.; Oyama, H.; Yamaki, K.; Sakio, N.; Kashiwabara, K.; Kuroda, Y.; Ito, A.; Yokota, A.; Ikeda, N.; Kikura-Hanajiri, R.; Ueda, H.; Numazawa, S.; Yoshida, T.; Kobayashi, N. Derivatization-assisted immunoassays: application for group-specific detection of potent methamphetamine and amphetamine enantiomers. *Anal. Methods* **2022**, *14*, 2745−2753.

(5) Dragan, A. M.; Parrilla, M.; Sleegers, N.; Slosse, A.; Van Durme, F.; van Nuijs, A.; Oprean, R.; Cristea, C.; De Wael, K. Investigating the electrochemical profile of methamphetamine to enable fast on-site detection in forensic analysis. *Talanta* **2023**, *255*, No. 124208.

(6) Liu, N.; Fan, Y.; Ma, Z.; Lin, H.; Xu, J. Materials design and sensing mechanism of novel calix[6]arene composite for sensitively detecting amine drugs. *Chin. Chem. Lett.* **2020**, *31*, 2129−2132.

(7) Shen, Z.; Li, W.; Tang, W.; Jiang, X.; Qi, K.; Liu, H.; Xu, W.; Xu, W.; Zang, S.; Zhen, K.; Li, H.; He, Q.; Tu, M.; Cheng, J.; Fan, Z.; Fu, Y. Fluorophor Embedded MOFs Steering Gas Ultra-Recognition. *Adv. Funct. Mater.* **2024**, *34*, No. 2401631.

(8) Dai, J.; Ogbeide, O.; Macadam, N.; Sun, Q.; Yu, W.; Li, Y.; Su, B. L.; Hasan, T.; Huang, X.; Huang, W. Printed gas sensors. *Chem. Soc. Rev.* **2020**, *49*, 1756−1789.

(9) Jian, Y.; Hu, W.; Zhao, Z.; Cheng, P.; Haick, H.; Yao, M.; Wu, W. Gas Sensors Based on Chemi-Resistive Hybrid Functional Nanomaterials. *Nano-Micro Lett.* **2020**, *12*, No. 71.

(10) Jo, Y. M.; Jo, Y. K.; Lee, J. H.; Jang, H. W.; Hwang, I. S.; Yoo, D. J. MOF-Based Chemiresistive Gas Sensors: Toward New Functionalities. *Adv. Mater.* **2023**, *35*, No. e2206842.

(11) Wen, Y.; Wang, G. E.; Jiang, X.; Ye, X.; Li, W.; Xu, G. A Covalent Organic-Inorganic Hybrid Superlattice Covered with Organic Functional Groups for Highly Sensitive and Selective Gas Sensing. *Angew. Chem., Int. Ed.* **2021**, *60*, 19710−19714.

(12) Sempionatto, J. R.; Lasalde-Ramirez, J. A.; Mahato, K.; Wang, J.; Gao, W. Wearable chemical sensors for biomarker discovery in the omics era. *Nat. Rev. Chem.* **2022**, *6*, 899−915.

(13) Ma, S.; Xu, J. Nanostructured metal oxide heterojunctions for chemiresistive gas sensors. *J. Mater. Chem. A* **2023**, *11*, 23742−23771.

(14) Hossain, M. K.; Hendi, A.; Asim, N.; Alghoul, M. A.; Rafiqul Islam, M.; Hussain, S. M. S. Chemiresistive gas sensing using graphene-metal oxide hybrids. *Chem. - Asian J.* **2024**, *19*, No. 16.

(15) Wan, H.; Gan, Y.; Sun, J.; Liang, T.; Zhou, S.; Wang, P. High sensitive reduced graphene oxide-based room temperature ionic liquid electrochemical gas sensor with carbon-gold nanocomposites amplification. *Sens. Actuators, B* **2019**, *299*, No. 126952.

(16) Liu, Q.; Sun, Q.; Shen, J.; Li, H.; Zhang, Y.; Chen, W.; Yu, S.; Li, X.; Chen, Y. Emerging tetrapyrrole porous organic polymers for chemosensing applications. *Coord. Chem. Rev.* **2023**, *482*, No. 215078.

(17) Li, L.; Zhang, S.; Lu, Y.; Zhang, J.; Zhang, X.; Wang, R.; Huang, J. Highly selective and sensitive detection of volatile sulfur compounds by ionically conductive metal-organic frameworks. *Adv. Mater.* **2021**, *33*, No. 2104120.

(18) Lu, Y.; Zhang, S.; Dai, S.; Liu, D.; Wang, X.; Tang, W.; Guo, X.; Duan, J.; Luo, W.; Yang, B.; Zou, J.; Huang, Y.; Katz, H. E.; Huang, J. Ultrasensitive Detection of Electrolyte Leakage from Lithium-Ion Batteries by Ionically Conductive Metal-Organic Frameworks. *Matter* **2020**, *3*, 904−919.

(19) Wu, J.; Wu, Z.; Han, S.; Yang, B.-R.; Gui, X.; Tao, K.; Liu, C.; Miao, J.; Norford, L. K. Extremely deformable, transparent, and high-

performance gas sensor based on ionic conductive hydrogel. *ACS Appl. Mater. Interfaces.* **2019**, *11*, 2364−2373.
(20) Qin, Y.; Chen, Y.; Zhang, X.; Zheng, A.; Xia, Q. Ionic conductive, antidrying, and flexible organohydrogels suitable for pressure sensors and gas sensors. *ACS Appl. Electron. Mater.* **2023**, *5*, 2758−2768.
(21) Cui, X.; Xi, Y.; Tu, S.; Zhu, Y. An overview of flexible sensors from ionic liquid-based gels. *TrAC, Trends Anal. Chem.* **2024**, *174*, No. 117662.
(22) Jo, Y.-M.; Kim, D.-H.; Wang, J.; Oppenheim, J. J.; Dincă, M. Humidity-mediated dual ionic−electronic conductivity enables high sensitivity in MOF chemiresistors. *J. Am. Chem. Soc.* **2024**, *146*, 20213−20220.
(23) Zhang, G.; Jin, L.; Zhang, R.; Bai, Y.; Zhu, R.; Pang, H. Recent advances in the development of electronically and ionically conductive metal-organic frameworks. *Coord. Chem. Rev.* **2021**, *439*, No. 213915.
(24) Won, D.; Bang, J.; Choi, S. H.; Pyun, K. R.; Jeong, S.; Lee, Y.; Ko, S. H. Transparent Electronics for Wearable Electronics Application. *Chem. Rev.* **2023**, *123*, 9982−10078.
(25) Zhu, H.; Luo, W.; Ciesielski, P. N.; Fang, Z.; Zhu, J. Y.; Henriksson, G.; Himmel, M. E.; Hu, L. Wood-derived materials for green electronics, biological devices, and energy applications. *Chem. Rev.* **2016**, *116*, 9305−9374.
(26) Wang, Y.; Zhang, L.; Zhou, J.; Lu, A. Flexible and transparent cellulose-based ionic film as a humidity sensor. *ACS Appl. Mater. Interfaces.* **2020**, *12*, 7631−7638.
(27) Zhu, J.; Zhu, P.; Zhu, Y.; Ye, Y.; Sun, X.; Zhang, Y.; Rojas, O. J.; Servati, P.; Jiang, F. Surface charge manipulation for improved humidity sensing of TEMPO-oxidized cellulose nanofibrils. *Carbohydr. Polym.* **2024**, *335*, No. 122059.
(28) Dai, S.; Chu, Y.; Liu, D.; Cao, F.; Wu, X.; Zhou, J.; Zhou, B.; Chen, Y.; Huang, J. Intrinsically ionic conductive cellulose nanopapers applied as all solid dielectrics for low voltage organic transistors. *Nat. Commun.* **2018**, *9*, No. 2737.
(29) Zhang, J.; Sun, T.; Zeng, S.; Hao, D.; Yang, B.; Dai, S.; Liu, D.; Xiong, L.; Zhao, C.; Huang, J. Tailoring neuroplasticity in flexible perovskite QDs-based optoelectronic synaptic transistors by dual modes modulation. *Nano Energy* **2022**, *95*, No. 106987.
(30) R, R.; Thomas, D.; Philip, E.; Paul, S. A.; Madhavan, A.; Sindhu, R.; Binod, P.; Pugazhendhi, A.; Sirohi, R.; Tarafdar, A.; Pandey, A. Potential of nanocellulose for wastewater treatment. *Chemosphere* **2021**, *281*, No. 130738.
(31) Chen, Y.; Li, L.; Zhang, J.; Sun, T.; Zhang, X.; Zhang, S.; Huang, J.; Zou, Y. Tailored ionically conductive graphene oxide-encased metal ions for ultrasensitive cadaverine sensor. *Chin. Chem. Lett.* **2024**, *35*, No. 109102.
(32) Zhang, S.; Li, L.; Lu, Y.; Zhang, J.; Liu, D.; Hao, D.; Zhang, X.; Tian, L.; Xiong, L.; Huang, J. Chemical sensors based on ionically conductive metal−organic frameworks for selective cadaverine detection. *J. Mater. Chem. C* **2022**, *10*, 5497−5504.
(33) Xiong, C.; Li, L.; Yang, M.; Chen, Y.; Wang, L.; Xiong, L.; Huang, J.; Zou, Y. Rationally Designed Ionically Conductive Metal-Organic Frameworks for Ultrasensitive Methamphetamine Analogs Sensor. *Adv. Funct. Mater.* **2024**, *34*, No. 2316511.
(34) Ammu, S.; Dua, V.; Agnihotra, S. R.; Surwade, S. P.; Phulgirkar, A.; Patel, S.; Manohar, S. K. Flexible, all-organic chemiresistor for detecting chemically aggressive vapors. *J. Am. Chem. Soc.* **2012**, *134*, 4553−4556.
(35) Li, J.; Lu, Y. J.; Ye, Q.; Cinke, M.; Han, J.; Meyyappan, M. Carbon nanotube sensors for gas and organic vapor detection. *Nano Lett.* **2003**, *3*, 929−933.

https://doi.org/10.1021/acsomega.5c00235
ACS Omega 2025, 10, 17770−17776